Meteorology and Atmospheric Physics (2025) 137:18
https://doi.org/10.1007/s00703-025-01064-0

ORIGINAL PAPER

On double monsoon onset and its predictive signature

Vaibhav Tyagi[1] · Saurabh Das[1] · Sukanta Kumar Das[2] · Bipasha Paul Shukla[2]

Received: 22 July 2024 / Accepted: 15 January 2025 / Published online: 8 February 2025

Abstract

The Indian monsoon is a complex phenomenon that greatly impacts agriculture and the economy of the region. Understanding the dynamics of the monsoon onset and its accurate predictions with a longer lead time is essential for effective planning and management decisions. Double monsoon onset is characterized by an early monsoon-like condition leading to a "bogus" (or false) onset followed by a delayed real onset. The present study provides an in-depth analysis of the 2023 monsoon onset, which was delayed 7 days than the normal monsoon onset, with a particular focus on understanding the predictive signature of such double monsoon onset. The study focuses on the total precipitable water vapour (TPW) to discern the monsoon onset over Kerala (MOK). Further investigation into the nature of the 2023 monsoon onset reveals the formation of Madden–Julian Oscillations (MJO) and twin perturbations, influencing convective activity and sea surface temperatures (SSTs). Notably, a distinct bi-peak evolution of surface winds is observed during the 2023 monsoon onset, suggesting a double monsoon onset pattern. Detailed analysis of 54 years of historical data spanning from 1950 to 2003 also suggests significant changes in wind speed over the Western Arabian Sea (WAS) for the cases of double monsoon onset. Accordingly, an index, namely the Double Monsoon Identification Index (DMII), is proposed to identify the potential cases of double monsoon onset. The DMII successfully predicted historical double monsoon onset cases (between 1950–2003) with an accuracy (ACC) of 0.96, a probability of detection (POD) of 0.9, and a false alarm rate (FAR) of 0.1 and identified two new cases between 2004–2023. The study highlights the predictive potential of surface winds in anticipating the double monsoon onset with considerable lead time from the climatological onset date, aiding proactive measures and planning in response to monsoon variability.

Responsible Editor: Silvia Trini-Castelli.

✉ Saurabh Das
saurabh.das@iiti.ac.in; das.saurabh01@gmail.com

Vaibhav Tyagi
vaibhavtyagi7191@gmail.com

Sukanta Kumar Das
sukanta@sac.isro.gov.in

Bipasha Paul Shukla
bipasha@sac.isro.gov.in

[1] Department of Astronomy, Astrophysics and Space Engineering, Indian Institute of Technology Indore, Indore, Madhya Pradesh, India

[2] Space Applications Centre (SAC), Indian Space Research Organisation (ISRO), Ahmedabad, Gujarat, India

Graphical abstract

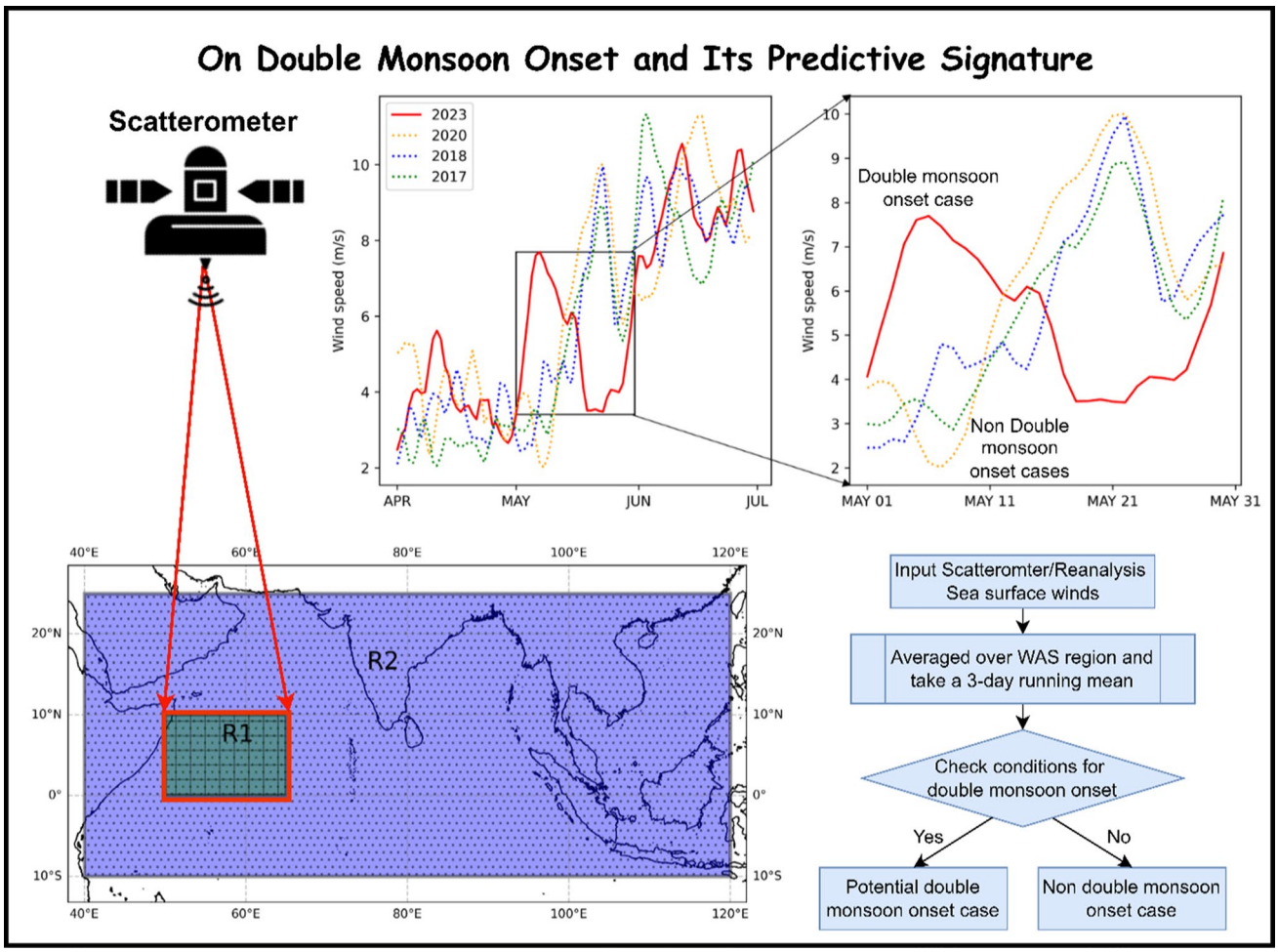

1 Introduction

The southwest monsoon is a seasonal weather pattern that brings heavy rainfall to the Indian subcontinent and neighbouring regions during the summer months from June till September (Ananthakrishnan et al. 1983 and Ananthakrishnan and Soman 1988; Parthasarathy et al. 1994). It typically sets in around June 1 (climatological onset date) over the Kerala coast with a standard deviation of about eight days and then gradually spreads northward covering the entire Indian peninsula and beyond (Maheshwar et al. 2017). The onset of monsoon over southern India (also known as monsoon onset over Kerala (MOK)) is considered the beginning of the rainy season during which India receives around 75% of the country's annual rainfall. The southwest monsoon, which plays a crucial role in the region's climate and ecosystems by replenishing water sources, sustaining agricultural productivity, and influencing various socio-economic activities, necessitates understanding its dynamics due to its significant impact on various sectors of the economy (Webster et al. 1998). A delayed or early onset of the monsoon can significantly impact various sectors of the country's economy (Wang et al. 2006; Gadgil and Rupa Kumar 2006); however, the date of MOK does not have a significant correlation with seasonal mean rainfall (Bansod et al. 1991). Nonetheless, studies suggest that the monsoon onset and crop planting dates are highly correlated, and even a 2-week delay significantly affects crop yields (Giné et al. 2008; Kala 2017).

Various methodologies, ranging from objective indices to subjective assessments by researchers and meteorological agencies, have been proposed to define monsoon onset dates, reflecting the complex nature of this seasonal transition (Rajan and Desamsetti, 2021; Joseph et al. 2015;

Puranik et al. 2013; Wang et al. 2009; Pai and Rajeevan 2009; Bhaskar et al. 2008; Kumar 2004; Xie et al. 1998; Ananthakrishnan and Soman 1988). Operationally, the India Meteorological Department (IMD) follows criteria (Pai and Rajeevan 2007 and 2009) based on rainfall, wind field and Outgoing Longwave Radiation (OLR) in order to declare the onset, defined as:

1. If after May 10, 60% of the stations (viz., Allapuzha, Amini, Kannur, Kochi, Kollam, Kottayam, Kozhikode, Kudulu, Mangalore, Minicoy, Punalur, Thalassery, Thiruvananthapuram and Thrissur) report rainfall of 2.5 mm or more for two consecutive days.
2. The depth of westerlies should be maintained up to 600 hPa in the box defined by 0–10° N and 55°–80° E and the zonal wind speed over the area bounded by 5°–10° N and 70°–80° E should be of the order of 15–20 Kts at 925 hPa.
3. The INSAT-derived OLR value should be below 200 W/m^2 in the box confined by 5°–10° N and 70°–75°.

Numerous studies have been conducted to understand the dynamics of southwest monsoon and its onset characteristics. The southwest monsoon is associated with the widespread rainfall over Kerala, which is fueled by moisture generated in the South Indian Ocean and transported to the Indian landmass by robust low-level cross-equatorial jet streams (Findlater 1969 and 1974; Joseph and Sijikumar 2004). The magnitude of these low-level jets (LLJs) is found to be highly correlated with the Indian Summer Monsoon Rainfall (ISMR) (Sagalgile et al. 2023). Researchers have extensively explored large-scale changes in circulation patterns, highlighting the development of a distinct band of deep convection characterised by low OLR values traversing in the east–west direction passing through the southern peninsula region (Ananthakrishnan et al. 1983; Pearce and Mohanty 1984; Ananthakrishnan and Soman 1988; Soman and Krishnakumar, 1993; Joseph et al. 1994 and 2006; Sikka and Gadgil 1980). Monsoon onset involves a steady buildup of moisture over the Arabian Sea and studies found that the Total Precipitable Water Vapour (TPW) peaks over the Western Arabian Sea (WAS) prior to the onset. It is also highly correlated with the MOK onset date (Simon et al 1994; Simon et al. 2006). Studies analysing scatterometer-derived surface winds indicate notable variations in surface winds and vorticity over the Arabian Sea within the Indian Summer Monsoon (ISM) region (Halpern et al. 1998; Rao et al. 1998; Sathiyamoorthy et al. 2012).

The Madden–Julian Oscillation (MJO), one of the dominant modes of intra-seasonal variability within the tropical atmosphere (Madden and Julian, 1972) plays a key role in monsoon onset (Baburaj et al. 2022a, b; Bhatla et al. 2017; Pai et al. 2011). Bhatla et al. (2017) have investigated the climatology of early and delayed onset of southwest monsoon in association with MJO. Their study suggests that strong MJO events are associated with the onset of summer monsoon over India, with MOK occurring mostly with MJO in phases 1, 2, 3, and 8. They also reported that MJO in phase 2 (phase 8) are associated with early (late) onset while in phase 1 and 3 associated with normal onset. An observational study by Taraphdar et al. (2018) highlights the interaction between seasonal background conditions and intra-seasonal variations linked to strong MJO activity in setting the summer monsoon onset. Their findings indicate that a delayed monsoon onset is often associated with the atmospheric circulation patterns of the leading dry phase of a strong MJO.

The occurrence of the Tropical Cyclones (TCs) in North Indian Ocean also influences the onset of the southwest monsoon by modulating the thermodynamical and dynamical state of the atmosphere. Studies in past suggest that during the active phase of the MJO over India Ocean and West Pacific region the conditions are more favourable for the development of TCs (Ho et al. 2006; Maloney and Hartmann 2001). A study by Baburaj et al. (2022b) shows that in recent decades the occurrence of TCs prior to the MOK has increased over Arabian Sea (AS) while decreased over Bay of Bengal (BoB). Baburaj et al. (2022a, b) examined the concurrent occurrence of Arabian Sea cyclones and the characteristics of the MOK across various MJO phases. Their findings indicate that MJO phase 1 is favourable for cyclogenesis over the AS, while phase 3 supports cyclone formation in both the AS and the BoB. In contrast, MJO phase 2 does not support cyclogenesis during the MOK.

The above discussions points to the fact that the ocean-atmosphere coupling plays a vital role in monsoon dynamics over the Indian monsoon region (Roxy et al. 2013; Athira and Abhilash 2021; Ahitra et al. 2020). The relationship between the various ocean–atmosphere interaction parameters are highly variable in space and time, which in some cases led to false detection of monsoon onset (Flatau et al. 2001 and 2003). Particularly, in early May, occasionally conditions resembling the monsoon may lead to a "bogus" or false onset, occurring a few weeks before the actual monsoon onset. This type of monsoon onset is known as "double monsoon" onset. For instance, the 2002 monsoon onset was a double onset, with IMD declaring onset on May 29 based on monsoon-like conditions, while the actual onset occurred on June 13 (Flatau et al. 2003; Puranik et al. 2013). Additionally, studies suggest that delayed onsets in such cases are associated with dry and hot weather across India (Wei-Dong et al. 2012; Flatau et al. 2001 and 2003). Like in 1995, a case of double monsoon onset, there were extremely hot conditions across various parts of India that resulted in deadly heat waves in early June (De et al. 1996; Halpert et al. 1996).

Fieux and Stommel (1977) first introduced the term ''multiple onset'' based on the analysis of surface winds from the ship reports from 1934 to 1972. They classify the onset into three categories, namely single, gradual, and multiple, based on the variation of the wind speed. Flatau et al. (2001) further delved into the dynamics of double monsoon onset, proposing a conceptual model [refer to Fig. 14 of the mentioned paper] and identifying the necessary conditions for its occurrence. Their findings highlighted two crucial conditions for the occurrence of a "bogus onset" followed by a delayed real monsoon onset: (i) the early May development of a Madden-Julian Oscillation (MJO), which triggers intense convection and decreases sea surface temperatures (SST) in the Bay of Bengal, and (ii) the subsequent propagation of the MJO into the Western Pacific and suppressed convection in the Indian Ocean by late May. While in past numerous studies have focused on the onset and predictability of the Southwest monsoon, studies related to the detection and prediction of double monsoon onsets remains limited. Given the vital role of timely and accurate monsoon onset prediction in agriculture, water management, and disaster preparedness, this gap underscores the importance of further investigation in this direction.

The central objective of the present study is to investigate the nature of the 2023 monsoon onset using various observational and reanalysis datasets. The present study also explored the predictability of the double monsoon onset and attempted to develop an objective criterion. The study investigates the predictive signature of double monsoon onset using surface winds from the scatterometer. The long-term ERA5 surface wind data from 1950 to 2003 is used to develop an index named Double Monsoon Identification Index (DMII). The proposed index is further implemented to the data from 2004 to 2023 to identify the double monsoon onset cases and prepared a climatology of such events. The paper is organized as follows: Section 2 provides an overview of the study area, details of the observational and reanalysis datasets employed in the study. Subsequently, the analysis of the nature of 2023 monsoon onset and the development of DMII index is presented in Section 3. Section 4 discusses the limitation and future scope of the present study. The summary and the key conclusions are presented in Section 5.

2 Study region, data and methods

2.1 Study area

The onset of the monsoon is a dynamic phenomenon influenced by various parameters, along with their spatial and temporal variations. Hence, the geographic domains were considered in this study based on previous literature to capture the spatio-temporal variability of key parameters, as depicted by R1 and R2 in Fig. 1. Simon et al. (1994, 2001) reported notable moisture changes over the Western Arabian Sea (WAS) region. A spatio-temporal analysis of monthly sea surface winds shows an increase over WAS starting in May, prior to the monsoon season (Rao et al. (1998); Sathiyamoorthy et al. (2012) and Tyagi et al. 2024). This led to the selection of region R1 (0°–10°N; 50°–65°E) to investigate the variations in total precipitable water (TPW)

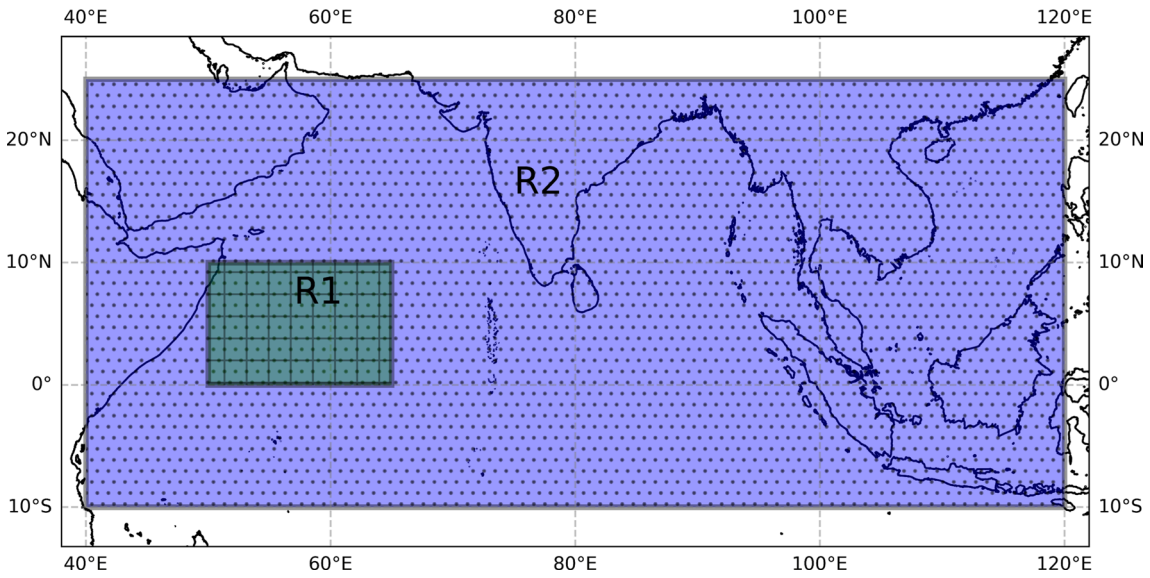

Fig. 1 Study map showing the extent of various geographical regions used to study the variation of different parameters. (R1: [0°-10° N; 50°-65° E], R2: [10° S-25° N; 40°-120° E])

and wind speed over WAS region. Region R2 (10°S–25°N; 40°–120°E) was chosen to study the variation in sea surface temperature (SST), surface winds, and outgoing longwave radiation (OLR) over the ISM region (Sathiyamoorthy et al. 2012). In this study, we do not explicitly examine the sensitivity of results to variations in the box area, especially concerning region R1. However, prior research has explored this sensitivity. Notably, Simon et al. (1994, 2001 and 2006) investigated the variation in TPW across multiple areas in the Indian Ocean, Arabian Sea, and Bay of Bengal. Their findings indicated a strong correlation between TPW peaks in the WAS—which corresponds to region R1 in this study—and the onset date of the MOK.

2.2 Data and methods

2.2.1 Scatterometer winds

The scatterometers are the side-looking radar onboard satellites. These are designed to estimate the wind speed and direction based on the measurements of the radar backscatter. Indian Space Research Organisation (ISRO) launched the Earth Observation Satellite, EOS-06 (Oceansat-03) on November 26, 2022, in a polar sun-synchronous orbit at 740 km altitude. It is third-generation satellite in Oceansat series. This is the successor of Oceansat-2 with improved payload specifications and added application areas. The present study utilises *daily analysed surface wind data* (Level 4 product) from the SCAT-03 sensor onboard the EOS-06 satellite. The dataset is obtained from the Meteorological and Oceanographic Satellite Data Archival Centre (MOSDAC) at a spatial resolution of 25 kms. The study focuses on the analysis of the pre-monsoon winds spanning May to June captured by the EOS-06 satellite for 2023. Additionally, available wind data from the SCATSAT-01 mission with similar sensor is used for comparative analysis for the years 2017–2018 and 2020. Though SCATSAT-01 was operational in 2019, but there was significant data missing during the period of interest and hence is not used in present study. The study uses the pentad (5-day average) evolution of the surface winds for 2023 over the region R2 to study the spatio-temporal variations of the surface winds. The 3-day running mean averaged over the region R1 (WAS) from April to the end of June was considered to study the temporal variation of the surface winds during the monsoon.

2.2.2 Total precipitable water vapor (TPW)

The Special Sensor Microwave Imager (SSM/I) is a near-polar orbiting satellite passive microwave radiometer onboard Defence Meteorological Satellite Program (DMSP) satellites since 1987. The TPW derived from the Special Sensor Imager (SSM/I) at 0.25×0.25 degree is used in the study. The mean TPW values are estimated from the gridded binary files considering the average of both ascending and descending passes over region R1. The data is obtained from the FTP site available at www.remss.com/missions/ssmi and analysed between March to June, 2023.

2.2.3 Outgoing long wave radiation (OLR)

The study also uses 1×1 degree daily interpolated OLR data to investigate the spatial characteristics of OLR over the ISM region. The data was accessed through the Thematic Real-time Environmental Distributed Data Services (THREDDS) Data Server (TDS), National Oceanic and Atmospheric Administration (NOAA). The study uses the time-longitudinal variation of the OLR averaged over the equatorial region (5° N–5° S) from January to June. Further, the pentad evolution of the OLR for 2023 is considered over region R2. To identify the presence of MJO, a 20–90-day bandpass Butterworth filter was applied to the unfiltered OLR data to isolate the 20–90-day frequency band characteristic of MJO, following Kiladis et al. (2014). Furthermore, MJO phase is identified for year 2023 using the real-time multivariate MJO index (RMM) data (Gottschalck et al. 2010) obtained from the Australian Bureau of Meteorology.

2.2.4 Sea surface temperature (SST)

The SST data from the Group for High Resolution Sea Surface Temperature (GHRSST) is obtained from the Earth data portal. The SST data available at 0.25-degree grid resolution is used to study the spatial pattern of the SST during the 2023 monsoon onset over region R2.

2.2.5 ERA5 reanalysis winds

The zonal (u) and meridional (v) components of surface winds from 1950 to 2023 are obtained from the European Centre for Medium Range Weather Forecasts (ECMWF) via the Copernicus climate data store available at a resolution of 0.25 degrees. The hourly gridded data is resampled as daily average data and the 3-day running mean of surface winds during the Southwest monsoon is analysed, averaged over region R1.

The datasets used in this study, including their spatial and temporal resolutions, periods of interest, and sources, are summarized in Table 1.

3 Results and discussion

3.1 Total precipitable water vapor (TPW)

Various studies found the TPW as an important parameter to study the MOK and found a strong correlation between the

Table 1 Summary of the various datasets used in the present study

Parameter	Spatial resolution	Temporal resolution	Year	Period of Interest	Source
Scatterometer surface winds	0.25×0.25 degree	Daily	2017–18, 2020, 2023	April to June	MOSDAC
Total precipitable water vapour (TPW)	0.25×0.25 degrees	Daily	2023	March to June	SSM/I
Outgoing Long Wave Radiation (OLR)	1×1 degree	Daily	2023	January to June	NOAA
Real-time multivariate MJO index (RMM)	–	Daily	2023	May	Australian Bureau of Meteorology
Sea surface temperature (SST)	0.25×0.25 degrees	Daily	2023	May—June	Earth data portal
ERA5 Surface winds	0.25×0.25 degrees	Hourly	1950—2023	April to June	Copernicus climate data store

peak TPW over WAS and MOK (Fasullo and Webster 2003; Simon et al. 2006; Ramesh Kumar et al. 2009). Beginning in March 2023, TPW was monitored in near real-time over the WAS, region R1, as shown in Fig. 1. Figure 2 illustrates the temporal evolution of the SSM/I derived daily TPW averaged over the WAS region, with the grey shaded region indicating the standard deviation (1σ). Analysis reveals a gradual increase in TPW from May 8, exceeding 50 mm and reaching its peak around May 11, consistently maintaining TPW values exceeding 50 mm until June 04. Notably, Fig. 2 depicts a dual peak in TPW around May 11 and 22. In general, TPW peaks over WAS approximately 18 ± 4 days preceding the MOK (Simon et al. 2006). Based on the analysis of peak TPW over WAS, we predict the onset dates for the 2023 MOK to be 18 days following the TPW peak, estimating them to be May 29 and June 09 with a deviation of plus or minus 4 days. The predicted onset date of June 09 closely aligns with the MOK date declared by IMD as June 08 (IMD report 2023).

The delayed onset as revealed by the TPW analysis raises our interest in further investigating the nature of the 2023 monsoon onset. By studying the temporal evolution and spatial distribution of key meteorological parameters, we further investigate various conditions that are essential for the double monsoon onset.

3.2 Formation of MJO and twin perturbations

MJO is an eastward-propagating system with alternating areas of increased and suppressed convection with a phase speed of around 5 m/s over the equatorial region (Madden and Julian, 1972 and 1994; Hendon and Salby, 1994; Zhang 2005; Straub 2013). The NOAA derived OLR (W/m^2) from January to June averaged over the equatorial region (from 5° N–5° S) is analysed to study the MJO activity. Figure 3 shows the time-longitude diagram of the OLR for the equatorial region. At the beginning of May, the equatorial convection developed around 60°E and further propagated in

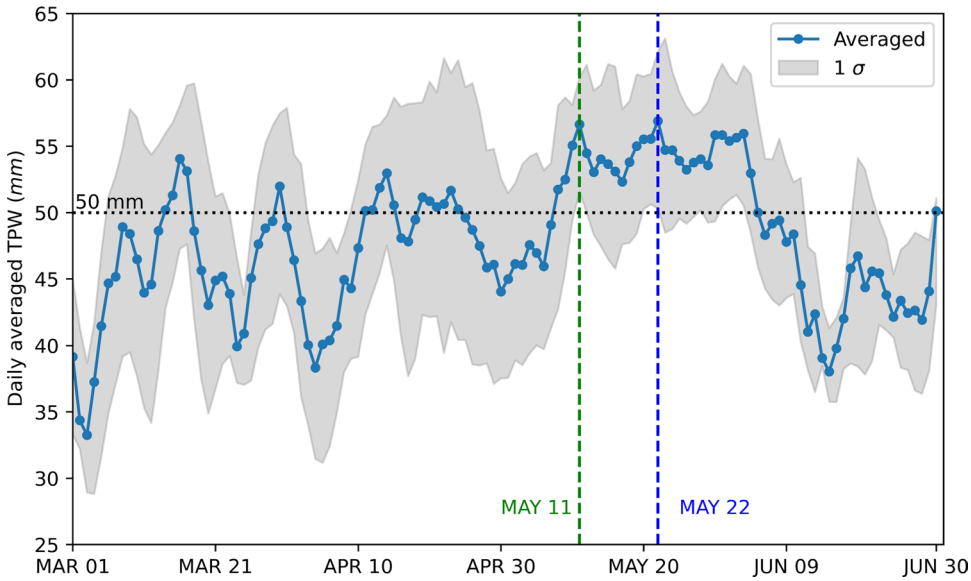

Fig. 2 Time series of SSM/I derived Total Precipitable Water Vapour (TPW) for 2023 averaged over WAS region from March 01 to June 30. (Shaded grey zone represent the 1σ level. The green and blue vertical dashed line corresponding to two peaks observed on May 11 and May 22.)

an eastward direction. In order to identify the presence of the MJO, a Butterworth bandpass filter is used to isolate the 20–90-day frequency band characteristic of MJO from unfiltered OLR data. Contour lines at −15 W/m^2 from the filtered OLR were overlaid on the unfiltered OLR plot to highlight regions of enhanced convective activity associated with the MJO. The MJO can be clearly seen in Fig. 3, represented by the black contour lines. As suggested by previous studies, the phase of the MJO also plays a crucial role in the monsoon onset. Accordingly, we have investigated the MJO phase during the 2023 monsoon onset. The MJO phase-space plot for May 2023 in Fig. 4 is generated using RMM data. A strong MJO in phase 8, represented by the blue curve extending outside the red circle in Fig. 4, was present in late May. This observation aligns with findings by Bhatla et al. (2017), which associated a strong MJO in phase 8 with delayed monsoon onset. Additionally, the occurrence of a strong MJO dry phase near the climatological onset may have contributed to the delay of 2023 onset seven days from the climatological onset date. This finding is also consistent with the analysis conducted by Taraphdar et al. (2018), which highlighted the impact of the MJO on monsoon onset, particularly its dry phase near the climatological onset date, causing delays due to surpassing background changes.

Further, the spatio-temporal characteristics of the convection over the AS and BoB are studied using the pentad evolution of OLR over region R2, as shown in Fig. 5. The May 1–5 pentad (5-day mean) clearly shows the development of

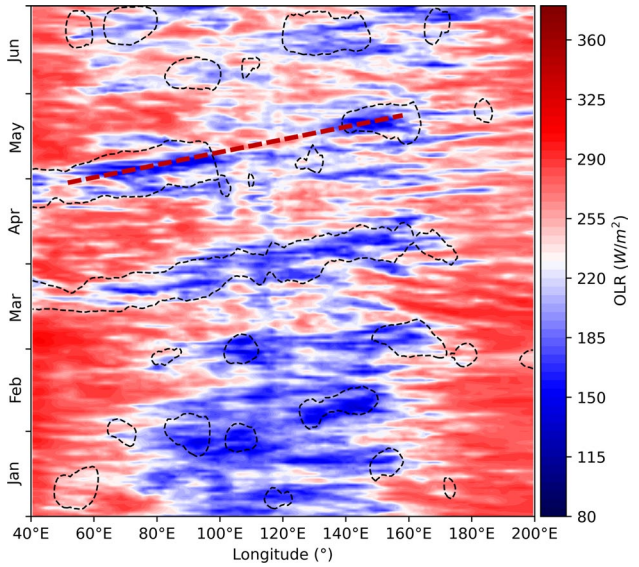

Fig. 3 Hovmöller diagram showing the time-longitudinal variations of NOAA-derived Outgoing Longwave Radiation (OLR) (W/m^2) from January to June, averaged over the equatorial region spanning from from 5° N–5° S. The black contour lines correspond to the intra-seasonal filtered OLR (20–90 days) as −15 W/m^2. The red dashed inclined line delineates the Madden Julian Oscillation (MJO)

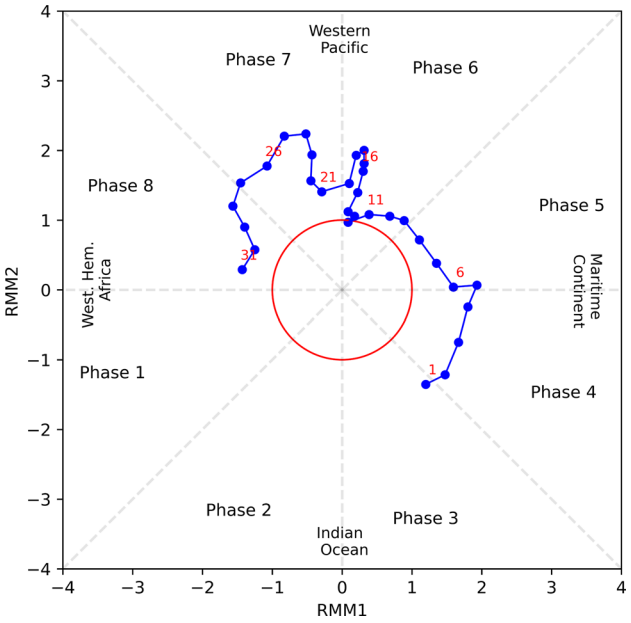

Fig. 4 The MJO phase-space diagram for May 2023. Red numbers indicate the day of the month in May. The unit circle centered at the origin distinguishes between strong and weak MJO phases. The blue curve outside the unit circle indicate strong phase of MJO

equatorial convection, and it further propagates to the southern BoB by May 6–10. This equatorial convection then splits into twin systems around the equator, as shown in Fig. 6a. Gill (1980) suggests that this breaking of equatorial convection into twin system around equator is the characteristic response of the heat source around the equator. Around May 11, two poleward moving systems can be observed: Mocha cyclone (OLR less than 120 W/m^2) moving in a northward direction and Fabien (OLR less than 180 W/m^2) moving towards the South. The lower values of the OLR indicate high convective activity. The corresponding Oceansat-03 surface winds from SCAT-03 capturing the twin systems are shown in Fig. 6b, with a higher wind speed exceeding 20 m/s observed at the centre of the Mocha cyclone. The observed warm SSTs over the BoB during the May 11–15 pentad, as depicted in Fig. 7, contribute to intensified convective activity creating monsoon-like conditions. Although there was no significant convection over the WAS (Fig. 5, May 11–15 pentad) around that time, the presence of strong sea surface winds of about 10–12 m/s (Fig. 8, May 11–15 pentad), as revealed by the pentad evolution of the scatterometer surface winds increased the evaporation. This phenomenon led to the accumulation of moisture in the atmosphere, consistent with the observed increase in TPW over the WAS peaking around May 11, with TPW values surpassing 50 mm, as illustrated in Fig. 2. The convective activity over BoB that also resulted in a cyclonic system, Mocha, notably reduced SSTs in the BoB during the May 16–20 pentad, as shown in Fig. 7. This

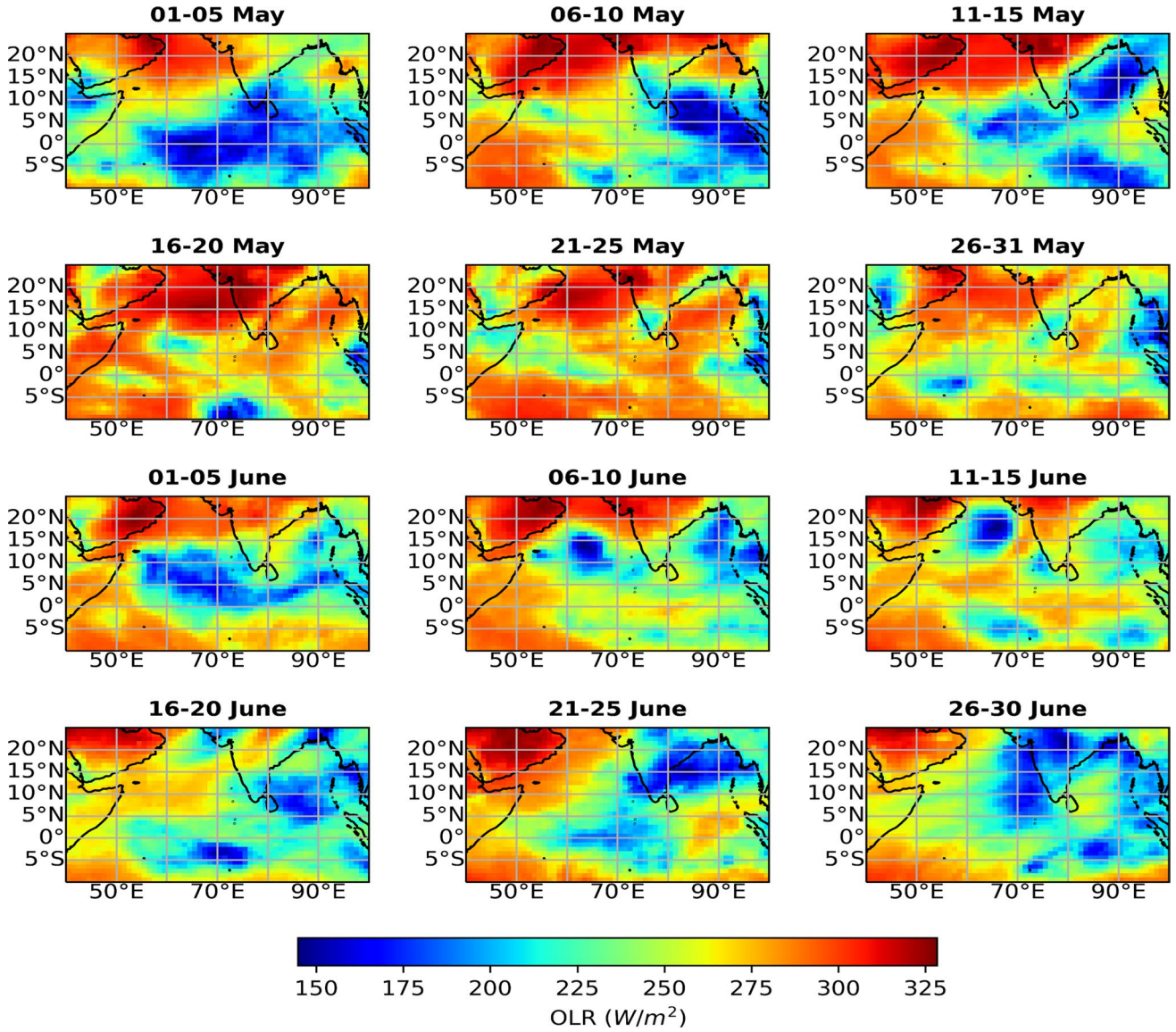

Fig. 5 Pentad evolution of NOAA derived Outgoing Longwave Radiation (OLR) (W/m^2) from May to June, over region R2, highlighting the spatio-temporal characteristics of convective activity

reduction in SSTs led to a decline in convection over the BoB as depicted in Fig. 5. Additionally, a decrease in wind speeds was observed over R1 during the same timeframe. Flatau et al. (2001) also investigated the change in large scale monsoon circulation using the monsoon Hadley (MH) index and observed significant changes during the same time. Previous studies suggest possible feedback mechanism deriving these changes (Rajendran et al. 2004 and Athira and Abhilash, 2021). Athira and Abhilash (2021) proposed a sequence of mechanisms involving "radiation-SST-wind-evaporation-SST gradient-wind stress-TPW-convection" responsible for setting the conditions responsible for MOK. Researchers have also examined the relationship between SST and precipitation, highlighting regional variations in the lagged response. Roxy et al. (2013) observed that, on average, precipitation lags SST by approximately 5 days over AS. However, over the BoB and the South China region, this lag extends to about 12 days. Subsequently, in early June, wind speeds over the WAS began to increase, reaching speeds of approximately 12–15 m/s coinciding with enhanced convection observed in both the AS and BoB. The analysis suggests that in 2023, bogus onset occurred approximately 3–4 weeks before the actual onset. The IMD officially declared the onset of the 2023 monsoon on June 08. 2023 monsoon exhibited a double monsoon onset pattern similar to a study conducted by Flatau et al. (2001; 2003). Therefore, the investigation suggests that the onset of the 2023 monsoon followed a "double monsoon onset" pattern.

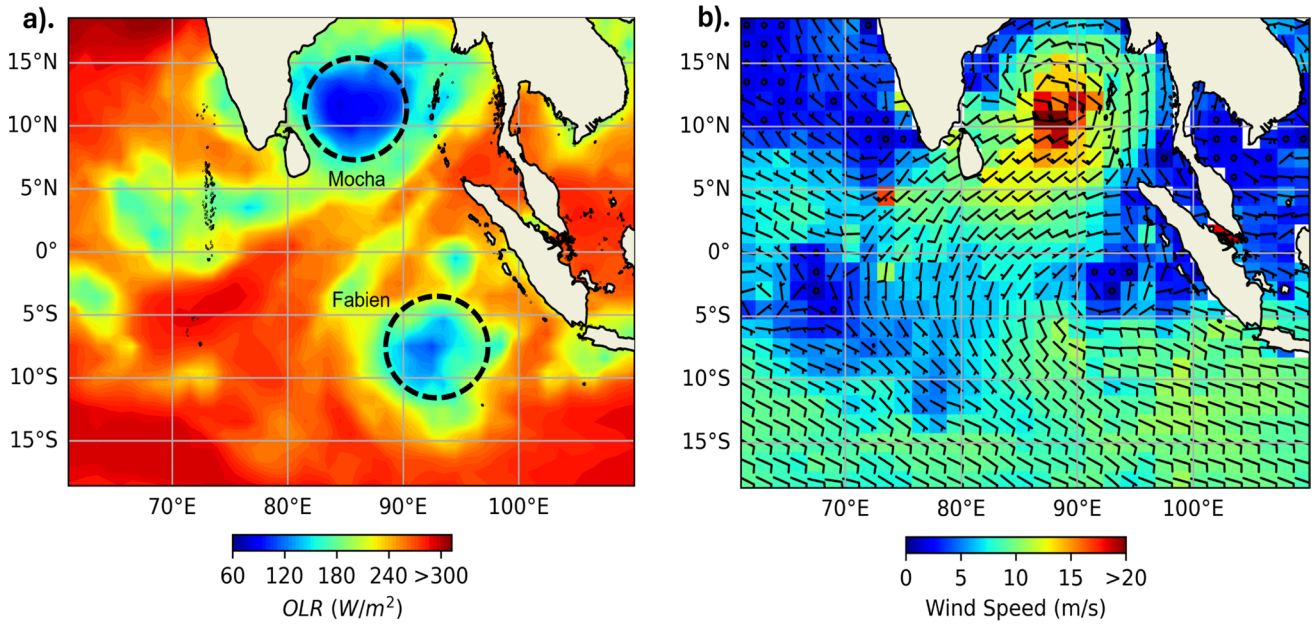

Fig. 6 **a** OLR snapshot on May 11 illustrating twin systems around the equator, with cyclones Mocha to the north and Fabien to the south. **b** Corresponding Scatterometer surface winds delineating the cyclonic structure of the systems

3.3 Predictive signature of the double monsoon onset

As discussed earlier, the double monsoon onset is associated with the "bogus onset," which delayed the real monsoon onset, and these double monsoon onsets are also associated with dry and hot weather conditions. This makes it important to understand the dynamics of these double monsoon onsets and identify their precursors or predictive signatures. The present study uses the daily analysed pre-monsoon winds (May–June) from SCAT-3 for the summer monsoon onset during the year 2023. The pentad evolution of surface winds reveals a consistent and substantial reversal in wind direction over the WAS, accompanied by a significant increase in cross-equatorial winds of about 10–12 m/s starting from the 01–05 May pentad, as shown in Fig. 8. Then the 16–20 May pentad reveals that the wind speed started decreasing until May 25 (lower than 5 m/s) and then started increasing again, reaching around 14 m/s prior to the actual monsoon onset. The pentad evolution of surface winds for 2023 reveals a distinct signature of the surface winds, highlighting an increase in wind speed in early May during the 2023 monsoon onset. This distinct nature of the 2023 monsoon onset (a "double monsoon onset" case) is further compared with the single monsoon onset cases to identify whether the signature is distinct from the single monsoon onset. As SCAT-03 was in operation only from April 2023, we used the scatterometer winds from its previous mission with similar sensor, which was SCATSAT-01. The available three years of daily analysed wind data for three single onset cases of 2017, 2018 and 2020 are used for this purpose. The MOK for these years occurs on May 30, May 29 and June 01, respectively. The data for 2019 was not used due to significant data gaps in the period of interest. Fig. 9 displays the daily surface winds averaged over region R1 for the years 2017, 2018, 2020, and 2023. A 3-day running mean is considered to eliminate the influence of the local disturbances. The time series of all single onset cases exhibits strong similarity and substantially different from that of double monsoon onset case of 2023 monsoon. A detailed look on May time series (Fig. 9) reveals that in the case of the 2023, the wind speed starts increasing in early May with significantly high values (~7 m/s), while it reaches its monsoon peak value of about 10–12 m/s by the end of May. The distinct nature of surface winds as observed in the 2023 monsoon onset was compared with historical cases of double monsoon onsets. The availability of long-term reanalysis data presents an opportunity for studying sea surface winds over an extended period. In this study, 74 years of ERA5 surface wind data from 1950 to 2023 were utilized. A comprehensive dataset was compiled based on available literature and onset dates declared by the IMD, as provided in Appendix 1 for reference. The long-term climatology of the MOK was examined from 1950 to 2023, revealing the inter-annual variability in the onset nature, depicted in Fig 10. The dataset was categorized into four groups: early onset, on-time onset, delayed onset, and double onset (a special case of delayed onset), determined relative to the climatological onset of June 01. Specifically, there were 40 instances of early onset, 5 instances of on-time onset, and 29 instances of delayed monsoon onset. Out of

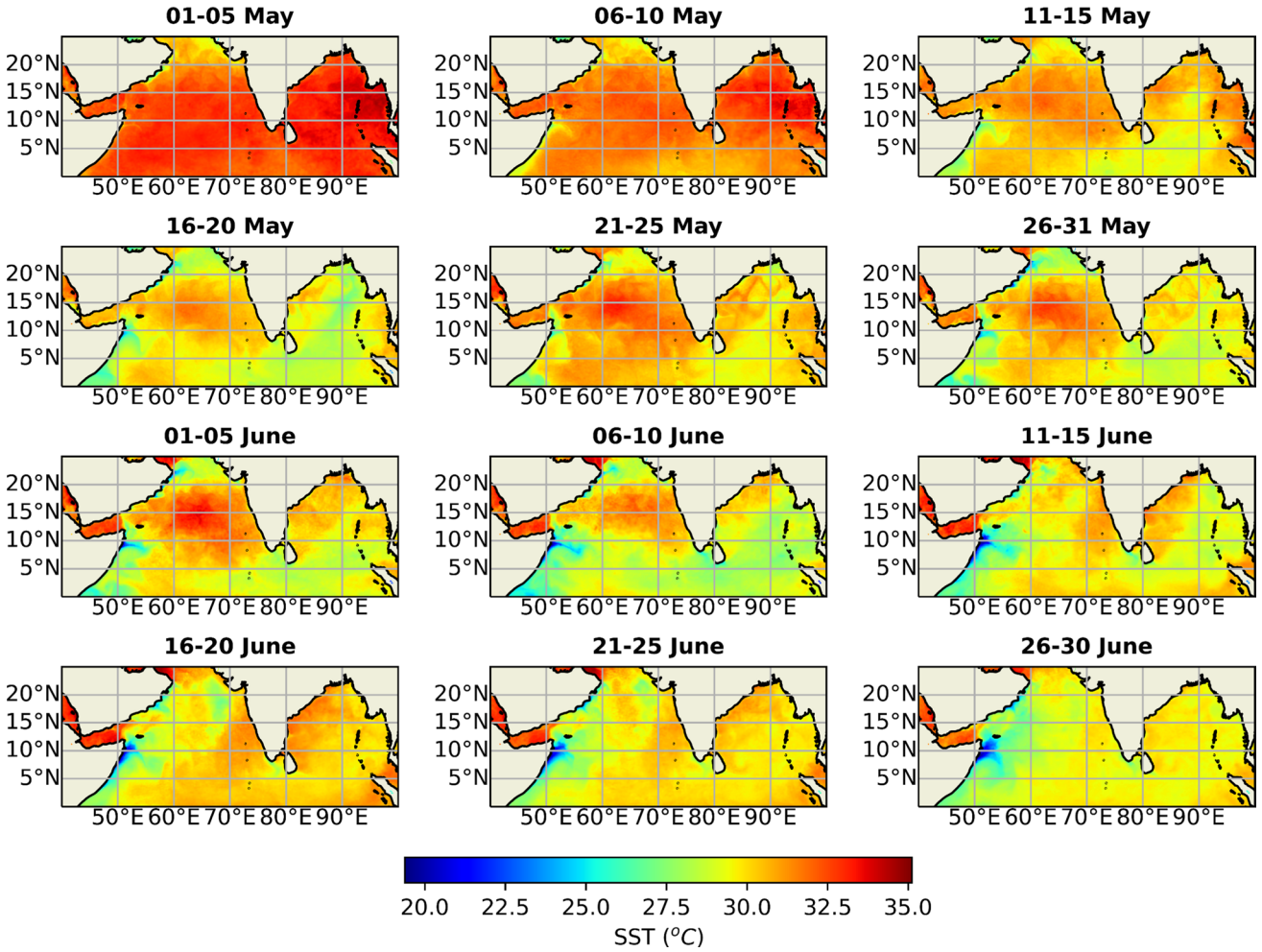

Fig. 7 Pentad evolution of GHRSST Sea Surface Temperature (in °C) from May to June over region R2

29 instances of delayed onset, 10 cases of double monsoon onset were identified, spanning from 1950 to 2003 (Flatau et al. 2001 and 2003; Fieux and Stommel 1977). Following those studies, there have been no known investigations specifically addressing the phenomenon of double monsoon onset. The list of all cases of double monsoon onset from 1950 to 2003 is presented in Table 2. Only the date of actual MOK is mentioned in Table 2 as the exact date of bogus onset for all cases are not documented in the literature. Nonetheless, the conditions associated with the bogus onset typically arise around three weeks before the climatological onset (Flatau et al. 2001).

Analysing the 3-day running mean of surface winds averaged over region R1, the study observed significant changes in wind speed during double monsoon onset years, as shown in Fig. 11. The black solid curve shows the variation of the surface winds, while the dotted blue curve shows the gradient of the surface winds. It is clear from Fig. 11 that in all the cases of double monsoon onset, there was a significant increase in the wind speed ($\geq$ 5 m/s, shown by the dashed green line), followed by a considerable decrease, before reaching its monsoon peak level in early June. Furthermore, significant changes in gradient were also observed during the double onset years, with the gradient extending beyond $\pm$ 0.5. However, for a few cases like 1968 and 1972, the early May increase in wind speed was not considerable, whereas there was a notable decrease in wind speed towards the end of May, consistently remaining below 5 m/s. Such cases were characterized by consistently low wind speeds ($<$ 5 m/s) throughout the month of May.

Fig. 11 illustrates the variations in surface winds during double monsoon onset cases. Additionally, surface wind analyses for all cases have been conducted and are provided in Figs. S1–S8 of the supplementary information. Among all the cases analysed, we observed two instances that exhibited patterns similar to double monsoon cases: the year 1977, which experienced an early onset, and 1983, which had a delayed onset. It is to be noted that 1983 monsoon onset was delayed, but it has not been reported as a double onset in the literature. Building upon these findings, we further

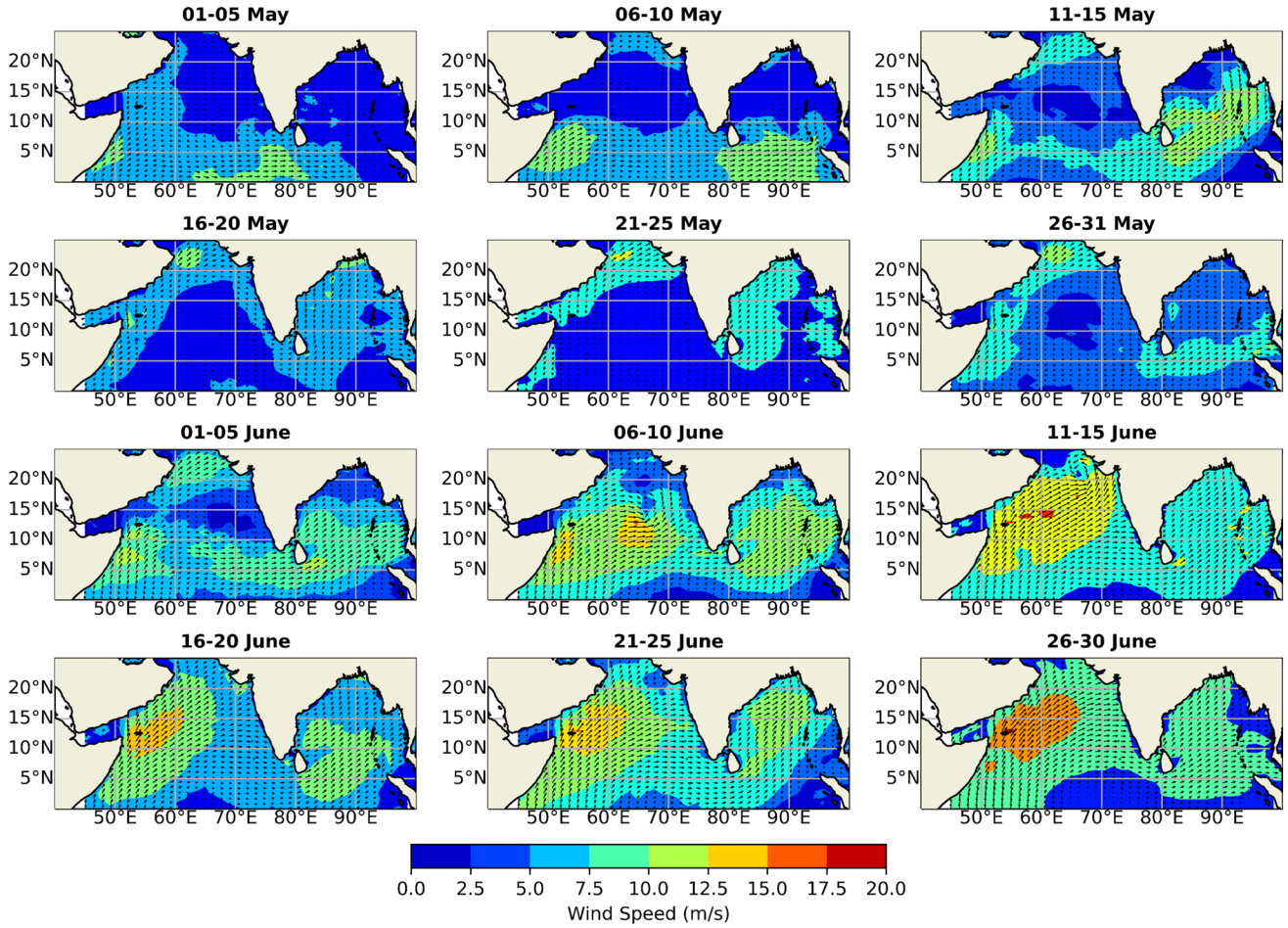

Fig. 8 Pentad evolution of EOS-06/Oceansat-03 Scatterometer sea surface winds (in m/s) from May to June over region R2, highlighting the spatio-temporal characteristics of wind field

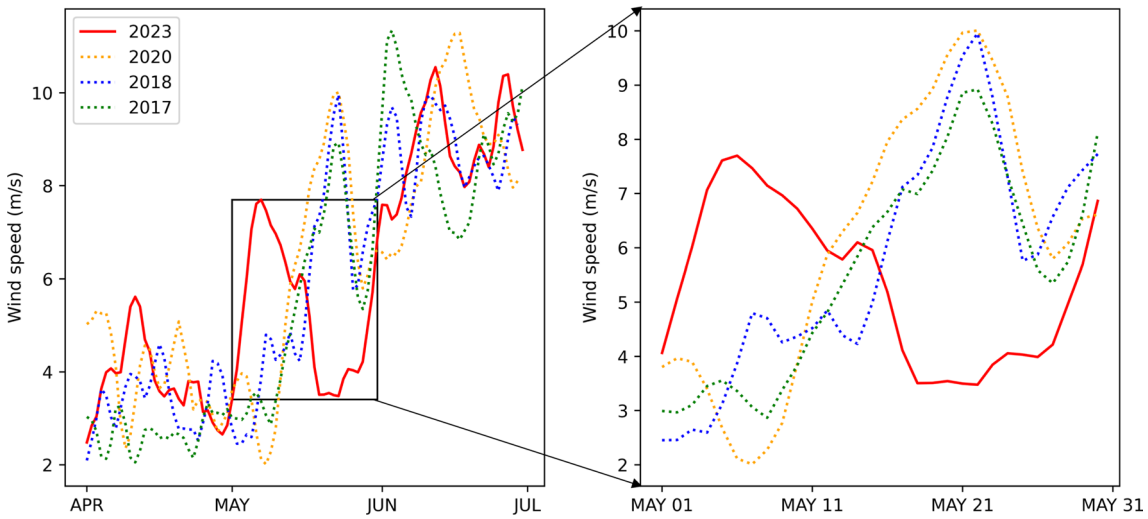

Fig. 9 Time series of Scatterometer surface winds averaged over region R1 from April to June for the years 2023, 2020, 2018, and 2017. The inset panel on the right provides a zoomed-in view of the wind speed variation during May

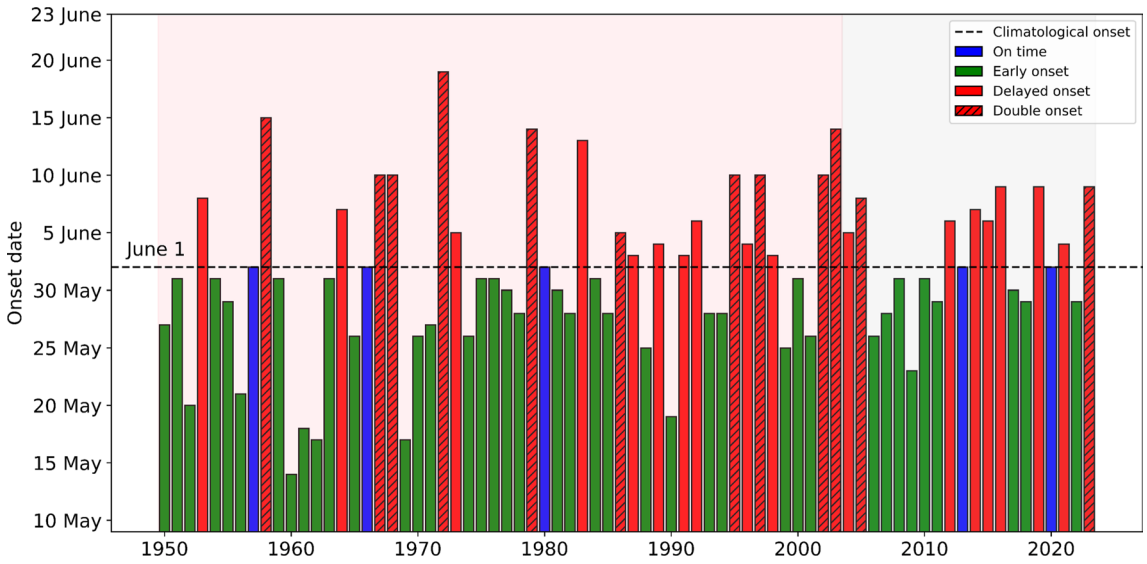

Fig. 10 Inter-annual variation of the monsoon onset dates over Kerala for 1950 to 2023

Table 2 List of historical double monsoon onset cases from 1950 to 2003 with corresponding onset dates. (J here refers to June, e.g. 14 J means 14 June)

Year	Onset date	Source
1958	14 J	Fieux and Stommel (1977)
1967	09 J	Flatau et al. (2001), Fieux and Stommel (1977)
1968	09 J	Fieux and Stommel (1977)
1972	18 J	Flatau et al. (2001)
1979	13 J	Flatau et al. (2001)
1986	04 J	Flatau et al. (2001)
1995	09 J	Flatau et al. (2001)
1997	09 J	Flatau et al. (2001)
2002	09 J	Flatau et al. (2003)
2003	13 J	Flatau et al. (2003)

aim to propose an index based on the variations of the surface winds over region R1. This index aims to identify the signature of double monsoon onset and predict the instances of double monsoon onset well in advance.

3.4 Development of Double Monsoon Identification Index (DMII)

3.4.1 Definition of DMII

The long-term ERA5 surface winds spanning from 1950 to 2023 is used for the development and validation of the DMII. The dataset was divided into two segments, one from 1950 to 2003, with the ten documented instances of double monsoon onset (as listed in Table 2) for the development of the DMII index. The other from 2004 to 2023 is used for validation and implementation purposes to establish a comprehensive climatology of all double-onset cases. To identify the cases of double monsoon onset, we propose an index derived from the analysis of ERA5 surface wind data spanning from 1950 to 2003. This index is defined as:

$$DMII = \left(\frac{WS - a_{thres}}{a_{thres}} \right) \quad (1)$$

where, WS represents the 3-days running mean of daily averaged wind speed over region R1 and a_{thres} is the threshold to detect the double monsoon onset.

Based on the analysis of 54 years of surface winds data we adopted the value of a_{thres} as 5 m/s. Figure 12 illustrates the variation of the DMII for all the double monsoon onset years, from May 1 to June 15. It was observed that cases with early May transition in DMII values, along with negative DMII values at the end of May, are associated with double monsoon onset. For the case of 2002, in the second half of May, negative DMII values were not observed as shown in Fig. 12. However, low DMII values indicated a significant break in wind speed during this period. To study the DMII variations for non-double monsoon cases, we have thoroughly examined the DMII variation for the years from 1950 to 2023. The variation of the DMII for all types of monsoon onset is presented in Figs. S9 to S16 in the supplementary information. It can be observed that for some cases of non-double monsoon onsets, only partial double monsoon onset conditions were met such as in 1992 and 1999. Furthermore, instances where DMII exhibited negative values throughout May were indicative of double monsoon onset, despite insufficient early May wind

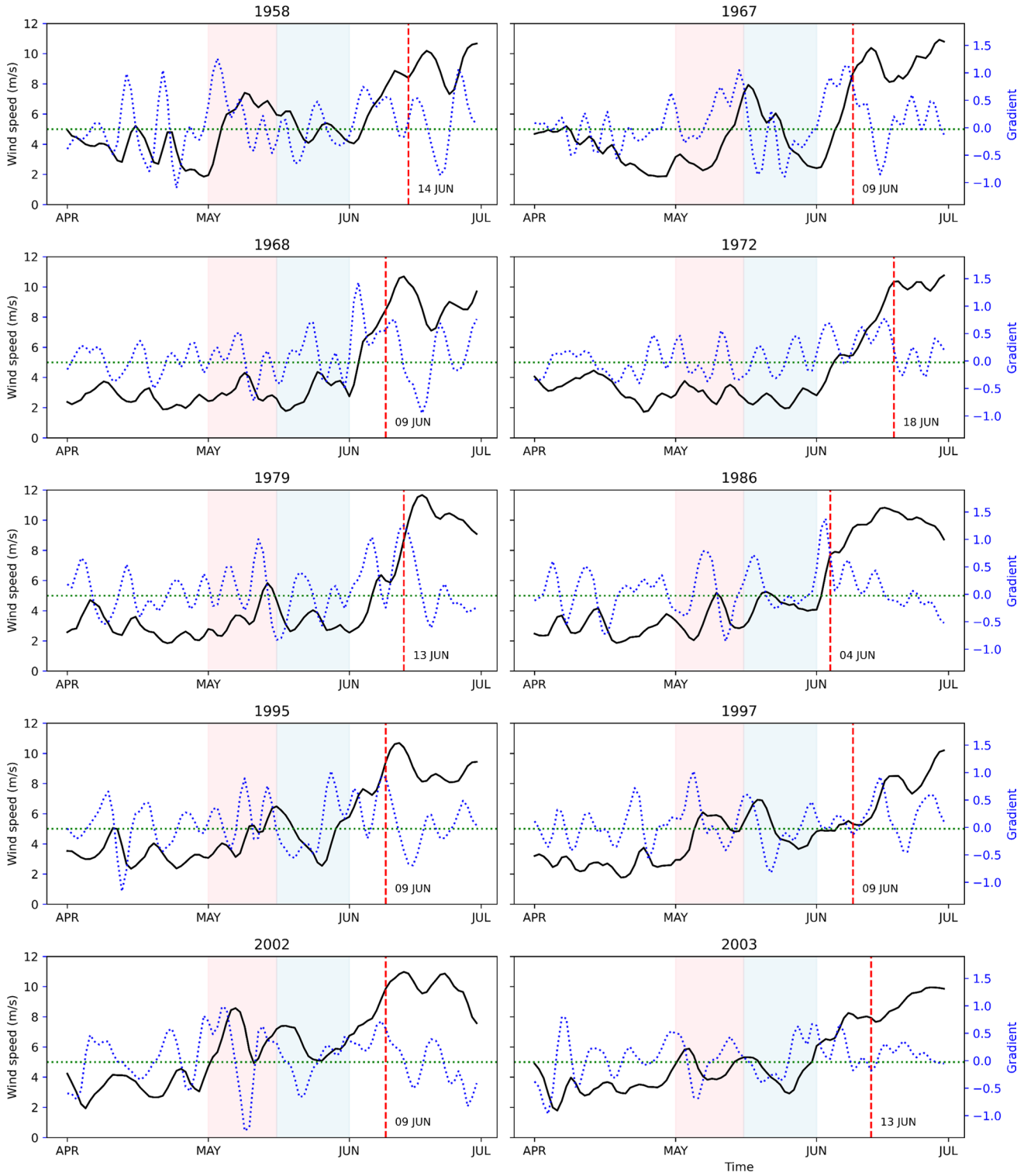

Fig. 11 Time series of ERA5 surface winds (black solid curve) averaged over region R1 from April to June for the cases of double monsoon years from 1950 to 2003. The gradient of the surface winds is shown with blue dotted curve. The onset date for each double monsoon event is marked with a corresponding red vertical line. Shaded areas highlight time periods with significant changes in wind patterns

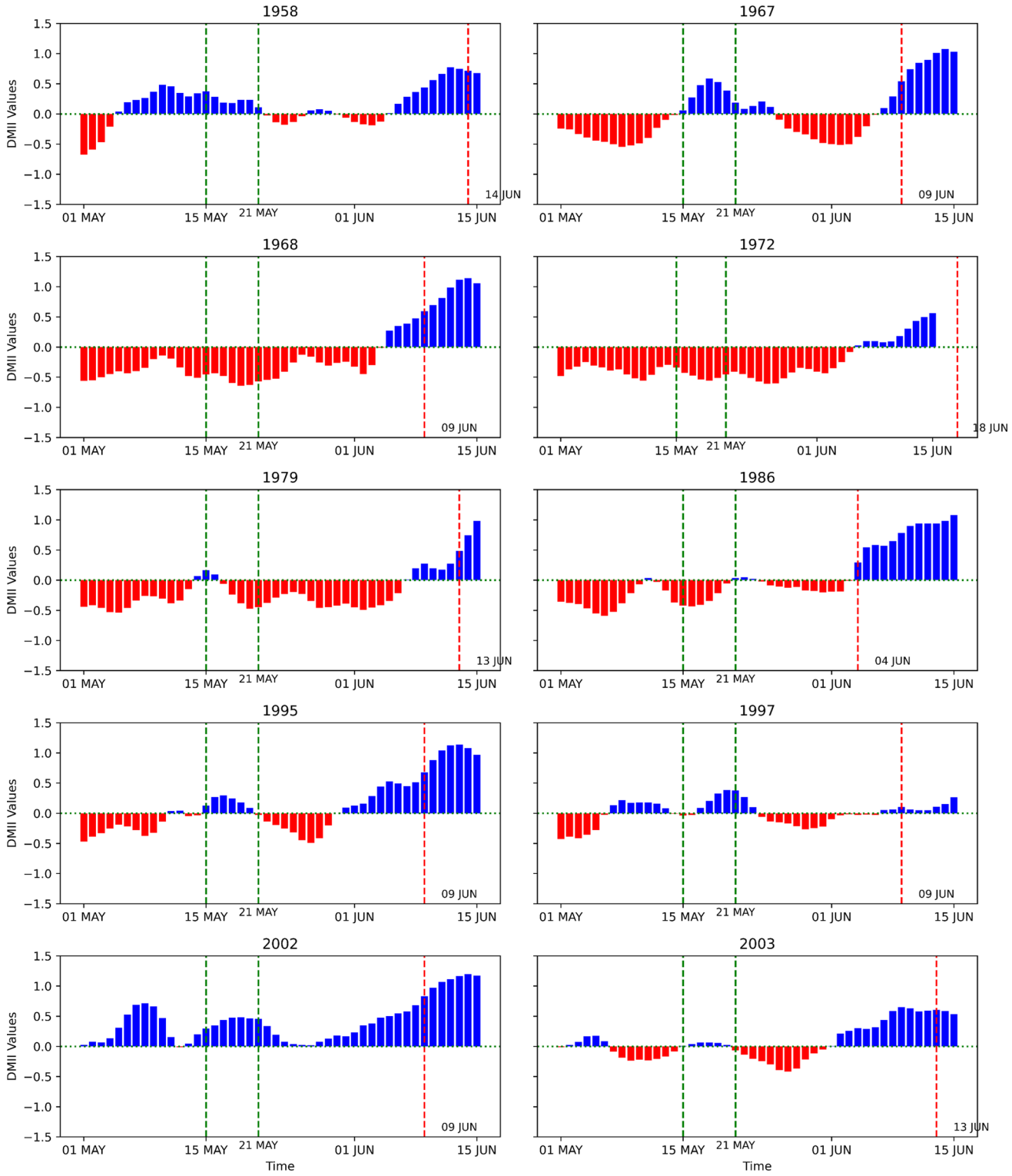

Fig. 12 Variation of the Double Monsoon Identification Index (DMII) for double monsoon onset cases from 1950 to 2003. Green vertical lines mark the reference dates of May 15 and May 21, while the red vertical lines represent the actual monsoon onset dates for each year. Blue bars indicate positive, and red bars indicate negative DMII values

speed increases. Thus, the analysis of the DMII reveals two distinct features observed in years characterised by double monsoon onset:

1. A transition from negative to positive DMII values in early May (first or second week) and a decrease in wind speed was observed, as depicted by negative DMII values towards the end of May.
2. Negative DMII values through May.

Based on these observations, a criterion was established to identify the potential cases of double monsoon onset. The criterion is defined as: "*Either an early May (before May 15) positive DMII, followed by negative DMII values for at least 5 consecutive days in the second half of May (after May 21) or negative DMII values throughout May*".

3.4.2 Sensitivity analysis of a_{thres}

To assess the robustness of the Double Monsoon Identification Index (DMII), a sensitivity analysis was conducted on the threshold parameter (a_{thres}). Various threshold values ranging from 3 m/s to 5.5 m/s were tested to evaluate their impact on the identification of double monsoon onset cases. For each threshold value, the DMII was calculated from 1950 to 2003, and its performance in identifying historical double monsoon onset events was assessed. The various skill scores were estimated, namely: accuracy (ACC), probability of detection (POD), false alarm rate (FAR), equitable threat score (ETS), and true skill statistic (TSS), as defined in Appendix 2. Figure 13 shows the variation of different skill scores with varying thresholds. ACC was about more than 80% for all cases; however, POD shows significant improvement as the threshold increases with a peak at 5 m/s. Also, the FAR showed a similar trend with a minimum FAR for 5 m/s. The TSS quantifies how effectively the forecast distinguishes between "yes" events and "no" events, showing a significant increase from 0.27 at 3 m/s to about 0.87 at 5 m/s. The ETS, measuring the accuracy of the forecast in predicting "yes" events compared to the observed "yes" events, also shows a similar trend. The poor skill score at the lower thresholds is due to their inability to capture the significant decrease towards the end of May. The sensitivity analysis suggests that the choice of the threshold parameter significantly influences the identification of double monsoon onset. Based on the analysis, a threshold value of 5 m/s was deemed optimal, striking a balance between sensitivity and specificity in detecting double monsoon-onset events. This threshold value demonstrated consistent performance across historical data, effectively capturing known instances of double monsoon onset while minimising false positives.

In this study, we focused only on the ISM and derived a 5 m/s wind threshold as a key indicator for identifying the double monsoon onset events over the WAS region. This threshold was established after extensive analysis of long-term wind data, however, the monsoon dynamics vary significantly across different regions, such as Southeast Asia, where distinct atmospheric and oceanic interactions may influence the monsoon's behaviour. Therefore, the 5 m/s threshold applied in this study may not be universally applicable to other monsoon systems and needs further study for other regions.

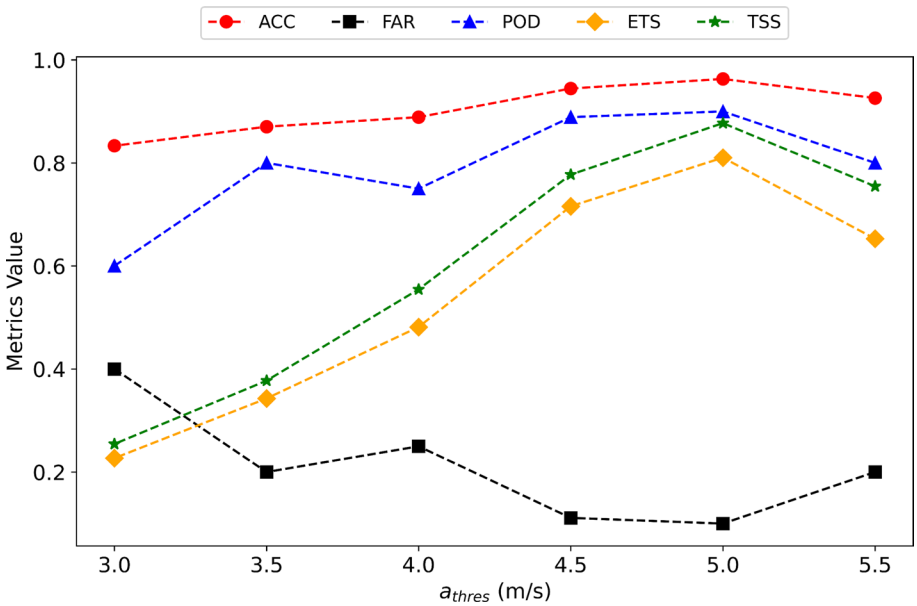

Fig. 13 The variation of different skill score for different a_{thres} values

3.4.3 Climatology of double monsoon onset

The criterion defined above was applied to the years from 2004 to 2023 to identify all the cases of double monsoon onset. It was found that the 2005 and 2023 monsoons were identified as double monsoon onset, which were both delayed by 7 days from the climatological normal onset date of June 01. The DMII variation for these years is shown in Fig. 14. As revealed by the analysis in Section 3.2, the double monsoon onset nature of the 2023 monsoon, the DMII successfully detected its double monsoon onset nature. After showing positive DMII values in early May (starting from May 4), the DMII values remained consistently negative for over 5 days after May 21, leading to the accurate identification of the 2023 monsoon as exhibiting a double monsoon onset pattern by May 25. This predictive capability provides a 5-day lead time before the normal climatological onset, enhancing preparedness and decision-making processes. Over a period of 74 years from 1950 to 2023, a total of 12 double monsoon onset cases were identified for the years 1958, 1967, 1968, 1972, 1979, 1986, 1995, 1997, 2002, 2003, 2005 and 2023.

Furthermore, in order to understand if the frequency of these events has changed over time, we conducted a decadal trend analysis. We have analysed the frequency of different type of monsoon onset cases between 1950 and 2020 and found no significant trends in the frequency of these events over time. However, it is important to note that the total number of monsoon onset cases analysed was 70, which presents a limitation for drawing robust conclusions from the statistical point of view. The relatively small sample size may also affect the reliability of the trends observed, particularly for specific categories like double onsets, where only 12 events were recorded (10 from 1950 to 2020 as used in this trend analysis).

4 Limitations and future scope

While the proposed index DMII has shown good predictive accuracy for identifying double monsoon onset cases, there are several limitations to consider. The index is based on threshold-based methods specifically tailored to the ISM region, and its application is context-dependent. The monsoon system is highly dynamic, and its behaviour is influenced by a range of complex factors such as climate variability and change that may affect threshold adapted. The DMII can successfully identify and predict the case of double monsoon onset, however, it is important to note that the current version of the index does not have the capability to predict the exact onset dates for such cases. One limitation stem from the fact that double monsoon onset cases are rare, leading to a relatively small sample size for index validation. This limited number of cases introduces a challenge in ensuring the robustness of the index under varying conditions.

As observed in present study and also reported by previous researchers (Flatau et al. 2001) that in case of multiple onsets, the convection in AS lagged behind the convection in BoB. Incorporating additional air-sea interaction parameters in DMII will further enhance its capability. In future work, it would be beneficial to explore a broader set of environmental and atmospheric parameters in addition to the wind speed. This may help to predict the actual beginning of the delayed onset dates for such events.

Another important aspect affecting monsoon are the occurrences of the TCs in North Indian Ocean (NIO). In the context of double monsoon onset, Flatau et al. (2001) highlights the development of the twin tropical depression in BoB on both sides of equator in early May. We have also observed the development of Mocha cyclone during May 2023, however there was no cyclogenesis in the AS during that period. This points towards the importance of cyclogenesis in different region in context of double monsoon onset and require further investigation.

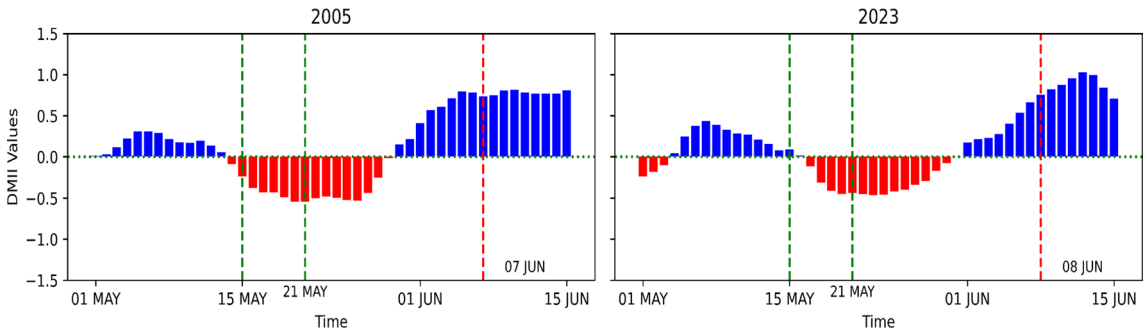

Fig. 14 Variation of the DMII for the year 2005 and 2023. Green vertical lines mark the reference dates of May 15 and May 21, while the red vertical lines represent the actual monsoon onset dates for each year. Blue bars indicate positive, and red bars indicate negative DMII values

A study by Patwardhan et al. (2014) examines the impact of climate change on monsoon onset under various scenarios and finds that climate models simulate an early monsoon onset towards the end of present century (2071–2100). Similar numerical studies can be planned to investigate the evolution of double monsoon onset cases under different climate scenarios and how external climatic factors such as El Niño or La Niña influence these events. However, the present study is mostly focused on understanding the signature in wind speed and this can be taken as future exercise.

5 Summary and conclusion

The onset of the monsoon is a pivotal event with extensive consequences for agriculture, water resources, and livelihoods throughout the region. Accurate prediction and understanding of the underlying dynamics are essential for proactive decision-making, resource allocation, and disaster preparedness. This study offers a thorough analysis of the atmospheric and oceanic factors shaping the MOK, particularly in context of Double Monsoon Onset with a special emphasis on 2023 monsoon onset. The study further analyzes various parameters and necessary conditions for the development of the double monsoon onset during the 2023 monsoon, as described by Flatau et al. (2001, 2003). The study reveals the double monsoon onset nature of the 2023 monsoon, with a bogus onset on May 11, followed by the real onset around June 8.

The TPW variations over the WAS region were found to be an important precursor of the monsoon onset that results in peak TPW values around 18 days prior to monsoon onset (Simon et al. 1994, 2006). However, for the case of 2023 monsoon onset, we observed the peak in TPW around May 11 associated with bogus onset much before the actual monsoon date. This results in the prediction date of 2023 monsoon onset as May 29, a false MOK. After few days when the monsoon-like conditions retract the TPW starts decreasing and again attains a peak around May 21. This results in the prediction of the 2023 onset to be on June 11, which is close to the onset date as declared by IMD. This deviation in the TPW pattern for 2023 highlights the challenges of relying solely on TPW for monsoon onset prediction, particularly in years with anomalous moisture buildup events. While TPW remains a valuable predictor in most cases, the occurrence of false peaks necessitates complementary predictors or adjustments to the methodology to account for such anomalies. The study investigated the predictive signature of the double monsoon onset that serves as an opportunity to identify such cases. Moreover, the DMII could be utilized alongside other objective criteria and indices. Combining it with existing indices and objective methods for MOK declaration could help reduce the likelihood of false monsoon onset declarations.

The double monsoon onsets result in the delay of the onset process and are often associated with the dry and hot conditions in India (Wei-Dong et al. 2012; Flatau et al. 2001 and 2003). The early prediction of such double monsoon onset cases is of great importance. The study emphasizes the significance of early warning predictions utilizing state-of-the-art instruments like scatterometers monitoring surface winds in near real time. The analysis of scatterometer surface winds proved instrumental in this context as they gave a unique signature of double monsoon onset in the case of 2023 onset. The study further investigates the long-term ERA5 surface winds data from 1950–2023 to understand the predictive signature of the surface winds in identifying the potential cases of double monsoon onset. Based on the long-term analysis of surface winds an index is defined to identify the potential cases of double monsoon onset called the "Double Monsoon Identification Index (DMII)". This is the first attempt to define an objective criterion to identify the potential cases of double monsoon onset. The interannual variation of the DMII is used to define a criterion to identify the double monsoon onset as: *"Either an early May (before May 15) positive DMII, followed by negative DMII values for at least 5 consecutive days in the second half of May (after May 21) or negative DMII values throughout May"*. The DMII successfully predicted historical double monsoon onset cases (between 1950–2003) with an accuracy (ACC) of 0.96, a probability of detection (POD) of 0.9, and a false alarm rate (FAR) of 0.1 and identified two new cases between 2004–2023. The DMII findings provide valuable predictive insights into the occurrence of double monsoon onsets with a lead of 5 days approximately from the climatological onset date i.e. around June 01, aiding in advanced forecasting and preparedness efforts for stakeholders in regions affected by monsoons. The DMII can successfully identify and predict the case of double monsoon onset, however, it is important to note that the current version of the index does not have the capability to predict the exact onset dates for such cases. Incorporating additional air-sea interaction parameters in DMII will further enhance its capability. In future work, it would be beneficial to explore a broader set of environmental and atmospheric parameters in addition to the wind speed.

Appendix 1

MOK onset dates dataset

The study analysed 74 years of monsoon onset over Kerala (MOK) from 1950 to 2023. The complete dataset of the onset date for 74 years is compiled from various sources,

including literature references and declarations by the Indian Meteorological Department (IMD) (R. P. Kane, 1980; Subrahmanyam et al. 2013) and is provided below for reference.

Year	Onset date	Year	Onset date	Year	Onset date
1950	27 M	1975	31 M	2000	31 M
1951	31 M	1976	31 M	2001	26 M
1952	20 M	1977	30 M	2002	09 J
1953	07 J	1978	28 M	2003	13 J
1954	31 M	1979	13 J	2004	04 J
1955	29 M	1980	01 J	2005	07 J
1956	21 M	1981	30 M	2006	26 M
1957	01 J	1982	28 M	2007	28 M
1958	14 J	1983	12 J	2008	31 M
1959	31 M	1984	31 M	2009	23 M
1960	14 M	1985	28 M	2010	31 M
1961	18 M	1986	04 J	2011	29 M
1962	17 M	1987	02 J	2012	05 J
1963	31 M	1988	25 M	2013	01 J
1964	06 J	1989	03 J	2014	06 J
1965	26 M	1990	19 M	2015	05 J
1966	01 J	1991	02 J	2016	08 J
1967	09 J	1992	05 J	2017	30 M
1968	09 J	1993	28 M	2018	29 M
1969	17 M	1994	28 M	2019	08 J
1970	26 M	1995	09 J	2020	01 J
1971	27 M	1996	03 J	2021	03 J
1972	18 J	1997	09 J	2022	29 M
1973	04 J	1998	02 J	2023	08 J
1974	26 M	1999	25 M		

(M (J) here refers to May (June), e.g. 27 M means 27 May.)

Appendix 2

Skill Score

The following skill score are calculated based on the below defined formula.

1. ACC (Accuracy)

$$ACC = \frac{a+d}{a+b+c+d}$$

ACC measures the proportion of accurate predictions, with a scale from 0 to 1, where 1 denotes perfect accuracy.

2. POD (Probability of Detection)

$$POD = \frac{a}{a+c}$$

POD measures the proportion of observed "yes" events that were accurately predicted, with scores ranging from 0 to 1, where 1 signifies perfect detection.

3. FAR (False Alarm Rate)

$$FAR = \frac{b}{a+b}$$

FAR measures the ratio of false alarms, which are instances where an event was predicted to occur but did not. It indicates the proportion of predicted events that turned out to be incorrect, providing insight into the tendency to overestimate events. The range of FAR is 0–1, as 0 is the perfect score.

4. ETS (Equitable Threat Score)

$$ETS = \frac{a - a_{random}}{a+b+c-a_{random}}$$

$$a_{random} = \frac{(a+b)\times(a+c)}{a+b+c+d}$$

ETS evaluates the accuracy of predicting "Yes" events compared to their actual occurrence, while considering hits that might happen by random chance. It ranges from −1/3–1, with 1 being a perfect score and 0 indicates no skill, a_{random} is the number of hits for random predictions.

5. TSS (True Skill Statistic)

$$TSS = \frac{a\times d - b\times c}{(a+c)\times(b+d)}$$

TSS gauges the effectiveness of a prediction in distinguishing between positive ("yes") and negative ("no") events; range of the TSS is −1–1, as 0 indicates no skill; and 1 indicates the perfect score.

where**,**

a = "hits" = number of times a "yes" prediction was followed by a "yes" occurrence

b = "false alarms" = number of times a "yes" prediction was followed by a "no" occurrence

c = "misses" = number of times a "no" prediction was followed by a "yes" occurrence

d = "correct non-events" = number of times a "no" prediction was followed by a "no" occurrence

Supplementary Information The online version contains supplementary material available at https://doi.org/10.1007/s00703-025-01064-0.

Acknowledgements We extend our sincere gratitude to the Meteorological and Oceanographic Satellite Data Archival Centre (MOSDAC/

SAC/ISRO) for providing access to the Oceansat-03 and Scatsat-01 daily analysed scatterometer surface winds. SSM/I and SSMIS data are produced by Remote Sensing Systems (available at www.remss.com/missions/ssmi). We also thank NOAA Climate Data Record for access to Daily Outgoing Longwave Radiation (OLR) data and to NASA Jet Propulsion Laboratory Physical Oceanography Distributed Active Archive Center for providing GHRSST Level 4 Sea Surface Temperature data. We are also grateful to the Copernicus Climate Change Service (C3S) for providing the ERA5 reanalysis data and to the Bureau of Meteorology Research Centre, Australia, for providing access to the RMM data. Financial support under the "Oceansat-3 Utilization Programme" by Space Applications Centre, (SAC) ISRO, India is acknowledged. One of the authors (SD) thankfully acknowledge financial support under MoES NARM Program (MoES/16/04/2021-RDESS/NARM-4) and SERB (CRG/2022/006986). One of the authors (VT) also thankful for the doctoral fellowship provided by the University Grant Commission (UGC). Authors are also thankful to the three anonymous reviewers for their valuable suggestions.

Author contributions Vaibhav Tyagi: Conceptualization, Material preparation, Data curation, Methodology, Formal analysis, Investigation, Writing—original draft and revision. Saurabh Das: Conceptualization, Methodology, Supervision, Writing—Review & Editing. Sukanta Kumar Das: Conceptualization, Writing—Review & Editing. Bipasha Paul Shukla: Conceptualization, Writing—Review & Editing.

Data availability All data used in this study are publicly accessible and already cited in Sect. 2.2.

Declarations

Conflict of interest The authors declare no conflict-of-interest.

References

Ananthakrishnan R, Pathan JM, Aralikatti SS (1983). The onset phase of the southwest monsoon. Curr. Sci., 52, 155–164. Available at https://www.currentscience.ac.in/Volumes/52/16/0755.pdf

Ananthakrishnan R, Soman MK (1988) The onset of the southwest monsoon over Kerala: 1901–1980. J Climatol 8(3):283–296. https://doi.org/10.1002/joc.3370080305

Athira UN, Abhilash S (2021) Ocean–atmosphere coupled processes in the tropical Indian Ocean region prior to Indian summer monsoon onset over Kerala. Clim Dyn 56(1):597–612. https://doi.org/10.1007/s00382-020-05499-6

Athira UN, Abhilash S, Sathiyamoorthy V (2020) Distinct atmosphere-ocean coupling processes on the onset phase of Indian summer monsoon during 2017 and 2018 as revealed through SCATSAT-1 and its comparison with CFSv2. Int J Remote Sens 41(20):8014–8033. https://doi.org/10.1080/01431161.2020.1767827

Baburaj PP, Abhilash S, Vijaykumar P, Nirmal CA, Mohankumar K, Sahai AK (2022a) Concurrent cyclogenesis in the northern indian ocean and monsoon onset over Kerala in response to different MJO phases. Atmos Res 280:106435. https://doi.org/10.1016/j.atmosres.2022.106435

Baburaj PP, Abhilash S, Nirmal CA, Sreenath AV, Mohankumar K, Sahai AK (2022b) Increasing incidence of Arabian Sea cyclones during the monsoon onset phase: Its impact on the robustness and advancement of Indian summer monsoon. Atmos Res 267:105915. https://doi.org/10.1016/j.atmosres.2021.105915

Bansod SD, Singh SV, Kripalani RH (1991) The relationship of monsoon onset with subsequent rainfall over India. Int J Climatol 11(7):809–817. https://doi.org/10.1002/joc.3370110707

Bhaskar Rao DV, Srinivas D, Ratna SB (2008) Regional scale prediction of the onset phase of the Indian southwest monsoon with a high-resolution atmospheric model. Atmos Sci Lett 9(4):237–244. https://doi.org/10.1002/asl.196

Bhatla R, Singh M, Pattanaik DR (2017) Impact of Madden-Julian oscillation on onset of summer monsoon over India. Theor Appl Climatol 128, 381–391. https://doi.org/10.1007/s00704-015-1715-4

De US, Desai DS, Bhandari SG (1996) HOT WEATHER SEASON (MARCH-MAY 1995). Mausam. https://doi.org/10.54302/mausam.v47i2.3731

Fasullo J, Webster PJ (2003) A hydrological definition of Indian monsoon onset and withdrawal. J Clim 16(19):3200–3211.

Fieux M, Stommel H (1977) Onset of the southwest monsoon over the Arabian Sea. Mon Wea Rev 105:231–236. https://doi.org/10.1175/1520-0493(1977)105%3c0231:OOTSMO%3e2.0.CO;2

Findlater J (1969) A major low-level air current near the Indian Ocean during the northern summer. Q J R Meteorol Soc 95:362–380. https://doi.org/10.1002/qj.49709540409

Findlater J (1974) The low-level cross-equatorial air current of the western Indian ocean during the northern summer. Weather 29(11):411–416. https://doi.org/10.1002/j.1477-8696.1974.tb04329.x

Flatau MK, Flatau PJ, Rudnick D (2001) The dynamics of double monsoon onsets. J Clim 14(21):4130–4146

Flatau MK, Flatau PJ, Schmidt J, Kiladis GN (2003) Delayed onset of the 2002 Indian monsoon. Geophys Res Lett. https://doi.org/10.1029/2003GL017434

Gadgil S, Rupa Kumar K (2006). The Asian monsoon—agriculture and economy. In The Asian Monsoon. pp. 651–683.

Gill AE (1980) Some simple solutions for heat-induced tropical circulation. Q J R Meteorol Soc 106(449):447–462. https://doi.org/10.1002/qj.49710644905

Giné X, Townsend RM, Vickery J (2008). Rational expectations? Evidence from planting decisions in semi-arid India. Bureau for Research and Economic Analysis of Development.

Gottschalck J, Wheeler M, Weickmann K, Vitart F, Savage N, Lin H, Higgins W (2010) A framework for assessing operational model MJO forecasts: a project of the CLIVAR Madden-Julian oscillation working group. Bull Am Meteorol Soc 91(8):1247–1258

Halpern D, Freilich MH, Weller RA (1998) Arabian sea surface winds and ocean transports determined from ERS-1 scatterometer. J Geophys Research: Oceans 103(C4):7799–7805. https://doi.org/10.1029/97JC02572

Halpert MS, Bell GD, Kousky VE, Ropelewski CF (1996) Climate assessment for 1995. Bull Amer Meteor Soc 77:S1–S43. https://doi.org/10.1175/1520-0477-77.5s.S1

Hendon HH, Salby ML (1994) The life cycle of the Madden–Julian oscillation. J Atmos Sci 51(15):2225–2237. https://doi.org/10.1175/1520-0469(1994)051%3c2225:TLCOTM%3e2.0.CO;2

Ho CH, Kim JH, Jeong JH, Kim HS, Chen D (2006) Variation of tropical cyclone activity in the South Indian Ocean: El Niño–southern oscillation and madden-Julian oscillation effects. J Geophys Res: Atmos. https://doi.org/10.1029/2006JD007289

IMD report. (2023). End of Season Report: Southwest Monsoon 2023.

Joseph PV, Sijikumar. (2004) Intraseasonal Variability of the low-level Jet stream of the Asian Summer Monsoon. J Climate 17:1449–1458

Joseph PV, Eicheid JK, Pyle RJ (1994) Interannual variability of the onset of the Indian summer monsoon and its association with the atmospheric features, El Nino and sea surface temperature anomalies. J Clim 7:81–105

Joseph PV, Sooraj KP, Rajan CK (2006) The summer monsoon onset over process over south Asia and an objective method for the date of monsoon onset over Kerala. Int J Climatol 26:1871–1893. https://doi.org/10.1002/joc.1340

Joseph S, Sahai AK, Abhilash S, Chattopadhyay R, Borah N, Mapes BE, Kumar A (2015) Development and evaluation of an objective criterion for the real-time prediction of Indian summer monsoon onset in a coupled model framework. J Clim 28(15):6234–6248. https://doi.org/10.1175/JCLI-D-14-00842.1

Kala N (2017). Learning, adaptation, and climate uncertainty: Evidence from Indian agriculture. MIT Center for Energy and Environmental Policy Research Working Paper, 23. Available at https://namratakala.com/wp-content/uploads/2020/01/kala_learning_dec2019.pdf

Kane RP (1980) Periodicities in the dates of onset of the southwest monsoon over Kerala. Mausam 31(3):461–464. https://doi.org/10.54302/mausam.v31i3.3797

Kiladis GN, Dias J, Straub KH, Wheeler MC, Tulich SN, Kikuchi K, Weickmann KM, Ventrice MJ (2014) A comparison of OLR and circulation-based indices for tracking the MJO. Mon Wea Rev 142:1697–1715. https://doi.org/10.1175/MWR-D-13-00301.1

Kumar MRR (2004) Forecasting of onset of southwest monsoon over Kerala coast using satellite data. IEEE Geosci Remote Sens Lett 1(4):265–267. https://doi.org/10.1109/LGRS.2004.832226

Madden RA, Julian PR (1972) Description of global-scale circulation cells in the tropics with a 40–50 day period. J Atmos Sci 29(6):1109–1123. https://doi.org/10.1175/1520-0469(1972)029%3c1109:DOGSCC%3e2.0.CO;2

Madden RA, Julian PR (1994) Observations of the 40–50-day tropical oscillation—a review. Mon Weather Rev 122(5):814–837.

Maheswar P, Rao AS, Ankur S, Ashish D, Kiran S, Shameera KS (2017) Prediction of Indian summer-Monsoon onset variability: a season in advance. Sci Rep 7(1):1–14. https://doi.org/10.1038/s41598-017-12594-y

Maloney ED, Hartmann DL (2001) The Madden–Julian oscillation, barotropic dynamics, and North Pacific tropical cyclone formation Part I Observations. J Atmos Sci 58(17):2545–2558

Pai DS, Rajeevan M (2007) Indian summer monsoon onset: variability and prediction. National Climate Centre, Indian Meteorological Department. Available at http://danida.vnu.edu.vn/cpis/files/Refs/Rainy_Season_Onset/Indian%20Summer%20Monsoon%20Onset-%20Variability%20and%20Prediction%20.pdf

Pai DS, Bhate J, Sreejith OP, Hatwar HR (2011) Impact of MJO on the intraseasonal variation of summer monsoon rainfall over India.Clim Dyn 36:41–55

Pai DS, Rajeevan M (2009) Summer monsoon onset over Kerala: New definition and prediction. J Earth Syst Sei 118:123–135. https://doi.org/10.1007/s12040-009-0020-y

Parthasarathy B, Munot AA, Kothawale DR (1994) All India monthly and seasonal rainfall series: 1871–1993. Theor Appl Climatol 49(4):217–224. https://doi.org/10.1007/BF00867461

Patwardhan S, Kulkarni A, Krishna Kumar K (2014) Impact of climate change on the characteristics of Indian summer monsoon onset. Int J Atmos Sci 2014(1):201695

Pearce RP, Mohanty UC (1984) Onsets of the Asian summer monsoon 1979–1982. J Atmos Sci 41:1622–1639

Puranik SS, Sinha Ray KC, Sen PN, Pradeep Kumar P (2013). An index for predicting the onset of monsoon over Kerala. Current Science, 954–961. https://www.jstor.org/stable/24098515

Rajan D, Desamsetti S (2021) Prediction of Indian summer monsoon onset with high resolution model: a case study. SN Appl Sci 3(6):645. https://doi.org/10.1007/s42452-021-04646-w

Rajendran K, Kitoh A, Yukimoto S (2004) South and East Asian summer monsoon climate and variation in the MRI coupled model (MRI-CGCM2). J Clim 17:763–782

Ramesh Kumar MR, Sankar S, Reason C (2009) An investigation into the conditions leading to monsoon onset over Kerala. Theoret Appl Climatol 95:69–82. https://doi.org/10.1007/s00704-008-0376-y

Rao UR, Desai PS, Joshi PC, Pandey PC, Gohil BS, Simon B (1998) Early prediction of onset of south west monsoon from ERS-1 Scatterometer winds. Proc Ind Acad Sci-Earth Planet Sci 107:33–43. https://doi.org/10.1007/BF02842259

Roxy M, Tanimoto Y, Preethi B, Terray P, Krishnan R (2013) Intraseasonal SST-precipitation relationship and its spatial variability over the tropical summer monsoon region. Clim Dyn 41:45–61. https://doi.org/10.1007/s00382-012-1547-1

Sagalgile A, Raju PVS, Kulkarni A, Prasad J, Rao VB, Fadnavis S (2023) Variability of low-level jet over the Arabian Sea and its association with Indian summer monsoon rainfall. Clim Dyn. https://doi.org/10.1007/s00382-023-07042-9

Sathiyamoorthy V, Sikhakolli R, Gohil BS, Pal PK (2012) Intra-seasonal variability in Oceansat-2 scatterometer sea-surface winds over the Indian summer monsoon region. Meteorol Atmos Phys 117:145–152. https://doi.org/10.1007/s00703-012-0189-5

Sikka DR, Gadgil S (1980) On the maximum cloud zone and the ITCZ over Indian longitudes during the southwest monsoon. Mon Weather Rev 108(11):1840–1853

Simon B, Joshi PC, Thapliyal PK, Pal PK, Sarkar A, Bhatia RC, Jain RK, Singh Devendra, Mukherjee SK, Gupta HV(2001) Monsoon onset monitored using multi-frequency microwave radiometer on-board Oceansat-1. Curr Sci81(6): 647–651

Simon B, Rayman SH, Joshi PC (1994) Determination of moisture changes prior to the onset of southwest monsoon onset over Kerala using NOAA/TOVS data. Meteorol Atmos Phys 53:223–231. https://doi.org/10.1007/BF01029613

Simon B, Rahman SH, Joshi PC (2006) Conditions leading to the onset of the Indian monsoon: a satellite perspective. Meteorol Atmos Phy 93:201–210. https://doi.org/10.1007/s00703-005-0155-6

Soman MK, Krishnakumar K (1993) Space–time evolution of meteorological features associated with the onset of Indian summer monsoon. Mon Weather Rev 121:1177–1194

Straub KH (2013) MJO initiation in the real-time multivariate MJO index. J Clim 26:1130–1151. https://doi.org/10.1175/JCLI-D-12-00074.1

Subrahmanyam MV, Pushpanjali B, Murthy KPRV (2013) Indian summer monsoon onset variations and consecutive rainfall over India. Ecol Environ Conserv 19:595–599

Taraphdar S, Zhang F, Leung LR, Chen X, Pauluis OM (2018) MJO affects the monsoon onset timing over the Indian region. Geophys Res Lett 45(18):10011–10018. https://doi.org/10.1029/2018GL078804

Tyagi V, Das S, Shukla BP (2024) Spatio-temporal analysis of long-term sea surface winds over the indian summer monsoon region. In IGARSS 2024-2024 IEEE International Geoscience and Remote Sensing Symposium (pp. 5976–5979). IEEE

Wang B, Ding Q, Joseph PV (2009) Objective definition of the Indian summer monsoon onset. J Clim 22(12):3303–3316. https://doi.org/10.1175/2008JCLI2675.1

Wang B, Gadgil S, Kumar KR (2006). The Asian monsoon—agriculture and economy. In The Asian Monsoon (pp. 651–683).

Webster PJ, Magana VO, Palmer TN, Shukla J, Tomas RA, Yanai M, Yasunari T (1998) Monsoons: processes, predictability, and prospects for prediction. J Geophys Res 103:14451–14510. https://doi.org/10.1029/97JC02719

Wei-Dong Y, Kui-Ping L, Jian-Wei SHI, Lin LIU, Hui-Wu W, Yan-Liang L (2012) The onset of the monsoon over the Bay of Bengal: The year-to-year variations. Atmos Ocean Sci Lett 5(4):342–347. https://doi.org/10.1080/16742834.2012.11447011

Xie A, Chung YS, Liu X, Ye Q (1998) The interannual variations of the summer monsoon onset over the South China Sea. Theor

Appl Climatol 59:201–213. https://doi.org/10.1007/s007040050024
Zhang C (2005) Madden-Julian Oscillation. Rev Geophys. https://doi.org/10.1029/2004RG000158